

## Exciton diffusion and dissociation in conjugated polymer/fullerene blends and heterostructures

A. Haugeneder, M. Neges, C. Kallinger, W. Spirkl, U. Lemmer, and J. Feldmann  
*Lehrstuhl für Photonik und Optoelektronik, Sektion Physik, Ludwig-Maximilians-Universität,  
 Amalienstraße 54, D-80799 München, Germany*

U. Scherf, E. Harth, A. Gügel, and K. Müllen  
*Max-Planck-Institut für Polymerforschung, Ackermann-Weg 10, 55128 Mainz, Germany*  
 (Received 13 October 1998)

We investigate the exciton dynamics in composite systems of conjugated polymers and fullerene molecules by photoluminescence (PL) and femtosecond transient absorption experiments. In solid mixtures (blends) we find a strong concentration-dependent quenching of the polymer PL. This is attributed to an efficient electron transfer (ET) from the photoexcited conjugated polymer to the fullerene. The ET dynamics is directly monitored by measuring the transient stimulated emission of the conjugated polymer. The transfer rate depends linearly on the  $C_{60}$  concentration and ranges between  $(66 \text{ ps})^{-1}$  and  $(5 \text{ ps})^{-1}$  for concentrations from 0.5% to 5%. This dependence is in accordance with an exciton diffusion process occurring prior to the ET. The exciton diffusion length in the conjugated polymer is directly determined by measuring the PL quenching in well-defined heterostructures comprising a self-assembled fullerene monolayer and a thin spin-coated polymer layer of variable thickness. From these measurements we infer a value of 14 nm for the exciton diffusion length in ladder-type poly (p-phenylene). Our results are of direct relevance for further optimization of polymer photovoltaic devices. [S0163-1829(99)07923-0]

### I. INTRODUCTION

Composite systems consisting of fullerenes and conjugated polymers have a large potential for applications in optoelectronic devices like, e.g., photodetectors and solar cells.<sup>1</sup> In such blend materials, charge-carrier generation is considerably enhanced in comparison to single component systems due to an electron transfer (ET) process that can occur after photoexcitation of the conjugated polymer. After completion of the transfer, the electron is located on the fullerene molecule while the hole (polaron) remains on the conjugated polymer. Due to the resulting spatial separation of the two charges, their Coulomb attraction is reduced compared to the primary photoexcitation, which is the intrachain exciton. As demonstrated in photocurrent and magnetic-resonance experiments, the ET leads to a much more efficient generation of charge carriers.<sup>2-4</sup>

Although there is ample evidence for a fast and efficient electron transfer in conjugated polymer/fullerene mixtures,<sup>5-7</sup> the microscopic mechanisms of the charge transfer have not been satisfactorily identified, i.e., the time-scale and the relevant distances that are involved in the ET have to be clarified. The delocalization length of the  $\pi$  electrons is of fundamental importance for a deeper understanding of the electronic properties of conjugated polymers. It also plays a crucial role for the ET. Vice versa a clarification of the ET process will also add to the knowledge about the conjugated polymer electronic properties.

A direct way to study the dynamics of the photoinduced ET is the investigation of the conjugated polymer excited state population—in semiconductor physics terms—the exciton density. The population  $N_{S_1}$  of the first excited singlet state  $S_1$  of the conjugated polymer is reduced by the ET. Concomitantly, the photoluminescence (PL) as well as the stimulated emission (SE) due to radiative transitions from the state  $S_1$  to the electronic ground state  $S_0$  are also

quenched. This opens up an optical way to detect the dynamics of ET. Furthermore, the stimulated emission can be directly observed in a time-resolved manner in femtosecond pump/probe-experiments and is therefore, a useful technique for studying the dynamics of ET directly.

Most of the experiments until now have been limited to the investigation of simple blend systems where the fullerene and the polymer are mixed in the same solvent and then spin cast into a thin-solid film. To understand the fundamental steps of the ET, the investigation of more defined systems, i.e., heterostructures, is needed.<sup>8</sup> One promising approach for a controlled deposition of well-defined heterostructures is the method of layer-by-layer adsorption.<sup>9</sup> In this technique, monolayers of a certain molecule are formed on an appropriate substrate by simply dipping into a solution containing the compound. This technique has been successfully used for the mono- and multilayer growth of differently charged polyions. We have recently extended this self-assembly (SA) technique for the preparation of monolayers of a suitably functionalized fullerene, namely fullerene carboxylic acid.<sup>10</sup>

In our contribution we report on a systematic study of the photoinduced ET in conjugated polymer/fullerene blend systems with gradually increasing fullerene concentrations and conjugated polymer/fullerene heterostructures. In our experiments, the ladder-type poly(p-phenylene) (LPPP) [see Fig. 1(a) for the chemical structure] is used as the conjugated polymer. By pump/probe experiments we measure the electron transfer dynamics directly. Even for fullerene concentrations as high as 5 wt % the ET is not instantaneous but can be time resolved via detection of the transient fullerene-induced depletion of the excited state. From our study we derive transfer times from 66 to 5 ps for weight concentrations ranging from 0.5% to 5%  $C_{60}$  in LPPP. Our data is in accordance with an exciton diffusion process occurring prior to the ET.

Direct evidence for diffusion is obtained from experi-

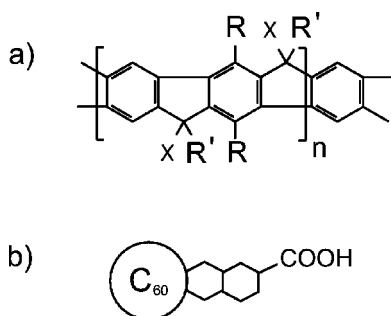


FIG. 1. Chemical structure of the compounds used for film fabrication. (a) The ladder-type poly(p-phenylene) conjugated polymer is deposited via spin coating. X represents a methyl-group and R and R' are *n*-hexyl and 1,4-decylphenyl, respectively. (b) The fullerene monolayer is deposited from a toluene solution containing a carboxy-functionalized C<sub>60</sub>-fullerene (C<sub>60</sub>H<sub>8</sub>O<sub>2</sub>).

ments on heterostructures comprising a self-assembled fullerene monolayer and an ultrathin spin-coated conjugated polymer layer. We find the polymer PL to be strongly quenched by the fullerene monolayer with a pronounced dependence on the thickness of the conjugated polymer film. The experimental data can be quantitatively understood within a simple model considering the diffusion of neutral excitations in the polymer. From the comparison of the experimental data with the model calculations, we derive a value of 14 nm for the exciton diffusion length in LPPP.

## II. EXPERIMENT

### A. Sample preparation

We use two sets of organic thin films in our experiments. As the first set of samples we have prepared simple blend systems by spin coating a toluene solution containing various relative concentrations of LPPP and the buckminsterfullerene. All films have the same optical density. Indium-tin-oxide (ITO) coated substrates were used in these experiments to avoid collective stimulated emission processes that occur in highly fluorescent conjugated polymers at high-excitation densities.<sup>11,12</sup> Due to the optical waveguide structure of the ITO-coated substrates, amplified spontaneous emission (ASE) leading to an ultrafast excited state depletion in LPPP is suppressed.<sup>13</sup> With the use of simple glass substrates ASE would obscure the observation of the ET processes under consideration.

Heterostructures of a spin-coated LPPP film on top of a fullerene monolayer deposited via SA were used as the second set of samples. We have utilized a carboxy-functionalized fullerene adduct, namely fullerene carboxylic acid (C<sub>60</sub>H<sub>8</sub>O<sub>2</sub>), prepared by Diels-Alder cycloaddition.<sup>14</sup> The chemical structure of this compound is shown in Fig. 1(b). The fullerene monolayer was deposited on a glass substrate after coating with a thin layer of poly(ethylenimine) (PEI). For depositing the fullerene monolayer the cleaned glass substrates were dipped into the PEI solution for 10 min, rinsed with pure water, spin dried, and then immersed into the fullerene solution. Apart from the simple preparation procedure, self-assembled monolayers offer the advantage of being adsorbed to the substrate. This leads to a more stable fullerene film than a thin evaporated C<sub>60</sub> film. For bilayers comprising an evaporated film interdiffusion of the two com-

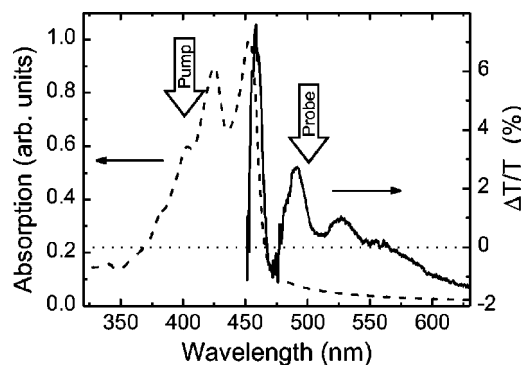


FIG. 2. The dashed line is the absorption spectrum of LPPP while the solid line are the transient absorption changes in LPPP at time delay zero after photoexciting with a femtosecond pulse having a pulse energy of 80 nJ at a wavelength of 400 nm. The arrows indicate the spectral positions of the pump pulse as well as the probe pulse used for a more detailed investigation of the excitation dynamics.

ponents might lead to rather ill-defined heterojunctions.<sup>15</sup> Thin LPPP films with thicknesses ranging from 5 to 65 nm were spin coated on top of the SA layer by varying the concentration of the LPPP solution and choosing the appropriate spin frequency. The polymer films were not intentionally oriented. There is, however, experimental evidence that the macromolecules close to the substrate are aligned in parallel to the surface with a random in-plane orientation.<sup>16</sup> The film thicknesses were measured using x-ray reflectivity and atomic force microscopy. In order to directly compare the influence of the fullerene molecules on the PL of the conjugated polymer we have only covered half of the substrate with the fullerene monolayer. Using this geometry, the polymer emission with and without an adjacent fullerene monolayer can be directly compared by simply moving the sample by a few millimeters (see inset in Fig. 5).

### B. Optical techniques

Our time-resolved optical experiments are performed with the output of a regeneratively amplified modelocked Ti:sapphire laser (*Spectra Physics Spitfire*) operating at a repetition rate of 1 kHz. For excitation of the polymer, we frequency double the femtosecond laser pulses at 800 nm. The laser beam is focused onto the sample with a spot diameter of 200 μm. The excitation densities are in the range of  $5 \times 10^{18} \text{ cm}^{-3}$ . The probe pulses for the transient absorption experiments are derived from a white-light continuum generated by focusing a small portion of the 800 nm output of the regenerative amplifier onto a sapphire crystal. The temporal resolution is approximately 200 fs and has been determined by two-photon absorption in zinc oxide. The chirp of the probe pulse has been characterized by the same method. For obtaining the differential transmission spectrum shown in Fig. 2 several spectra for different time delays were taken, followed by a numerical chirp correction. For the detailed investigation of the dynamics of the transmission changes a small portion of the white light was spectrally selected by an interference filter at a wavelength of 500 nm and a bandwidth of 10 nm. The pump-induced transmission changes of the probe beam were recorded with a photodiode and subsequent phase-sensitive amplification locked to the chopped

pump beam. The chopping frequency was set to half the repetition rate of the laser system. The polarization of the probe pulses was chosen to be orthogonal to the polarization of the pump pulses.<sup>17</sup> As excitation source for the time-integrated PL measurements we directly frequency double the output of the modelocked Ti:sapphire laser at a repetition rate of 82 MHz. Typical time-averaged excitation intensities on the sample are about 15 W/cm<sup>2</sup>. The emission spectra are recorded with a spectrometer and a subsequent charge-coupled-device (CCD) detector. All experiments were carried out at room temperature.

### III. RESULTS AND DISCUSSION

#### A. Electron transfer in LPPP/C<sub>60</sub> blends

The spectral positions of the pump and probe pulses are indicated in Fig. 2. The figure compares the absorption spectrum (dashed line) with the induced transmission changes immediately (time delay 0 ps) after pumping with a femtosecond laser pulse (solid line). The pump pulses at 400 nm excite vibronic progressions of the main  $S_1 \leftarrow S_0$  absorption band of LPPP, which is located at 453 nm. The most prominent features in the differential transmission spectrum are an enhanced transmission at the low-energy tail of the purely electronic transition at 460 nm as well as at the spectral positions of the vibronic side bands at 490 and 526 nm, respectively. For longer wavelengths, we observe a photoinduced absorption that can be attributed to a superposition of an  $S_n \leftarrow S_1$  excited state absorption and the absorption due to charged excitations (polarons) that are formed by spontaneous or trap-assisted dissociation of the neutral  $S_1$  state.<sup>18,19</sup>

For a detailed investigation of the charge-transfer dynamics, we use probe pulses centered at a wavelength of 500 nm with a bandwidth of 10 nm. These pulses are derived from the white-light continuum via spectral filtering. At this wavelength, the positive transmission change is optical gain due to stimulated emission from the vibronic ground state of the first excited electronic state  $S_1$  into a vibronically excited state of the electronic ground state  $S_0$ . The transmission change, being proportional to the density of excited states, is used to monitor the transient excited state population in the time-resolved experiments discussed below.

The basic observation of ET is manifested in the time-integrated PL spectra of LPPP/C<sub>60</sub> mixtures with different fullerene concentrations shown in Fig. 3. The uppermost curve represents the PL spectrum of undoped LPPP. The spectra for the C<sub>60</sub>-doped samples indicate that the polymer PL is efficiently quenched for increasing fullerene concentrations. No changes in the spectrum are observed as expected for a system where all the emission bands originate from the radiative decay of the same excited state. The inset displays the concentration dependent relative PL quenching  $\Delta I/I_0$  (with  $\Delta I$  being the PL-quenching and  $I_0$  representing the PL intensity of the undoped sample). At a concentration as low as 0.5% the PL is already reduced by almost 40%. For the highest concentration of 10 wt % the PL is reduced by more than 95% of the value for the undoped sample. This strong PL quenching is attributed to the ET, which occurs after photoexciting the conjugated polymer.

For a detailed study of the transfer dynamics we have carried out femtosecond stimulated emission (SE) measure-

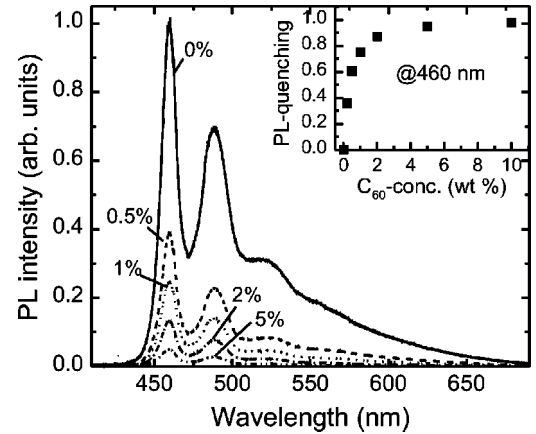


FIG. 3. PL-spectra of LPPP/C<sub>60</sub>-blends with various C<sub>60</sub>-concentrations. The samples were excited with femtosecond laser pulses at 400 nm. The inset shows the relative PL quenching at an emission wavelength of 460 nm.

ments. The transient SE for the LPPP films doped with various amounts of C<sub>60</sub> are depicted in Fig. 4. The maximum transmission change observed around time delay zero is identical for all C<sub>60</sub> concentrations. This indicates that no ET occurs within the time resolution of the system. The excited state dynamics for larger time delays changes notably upon doping with C<sub>60</sub>. The main observation is an accelerated decay for increasing fullerene concentrations. Additionally, a long-living component becomes more and more prominent. The latter observation is attributed to the buildup of photoinduced absorption due to dissociated charge-carrier pairs created by the ET.

After photoexciting with a femtosecond laser pulse, the transient population  $N_{S_1}$  of excited singlet states is described by the following rate equation:

$$\frac{\partial N_{S_1}}{\partial t} = -[k_0 + k_T(c)]N_{S_1} - \gamma N_{S_1}^2. \quad (1)$$

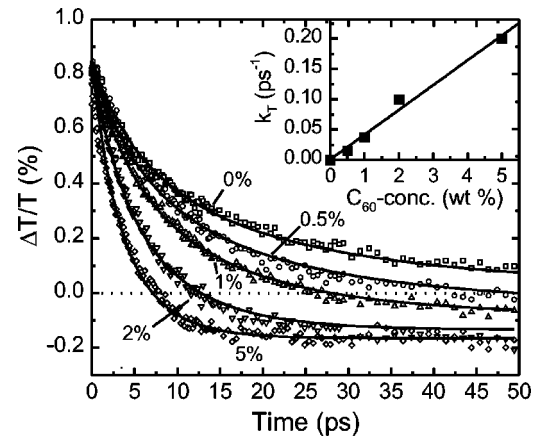


FIG. 4. Stimulated emission transients of LPPP/C<sub>60</sub> blends for various C<sub>60</sub> concentrations ranging between 0% and 5% (open symbols). The pump pulses have a duration of 150 fs and are centered at 400 nm. The probe pulses are derived from a white-light continuum by spectrally filtering ( $\lambda_0 = 500$  nm,  $\Delta\lambda = 10$  nm). The solid lines represent the results based on the fitting procedure described in the text. The deduced electron transfer rates are shown in the inset.

Here the first term on the right-hand side describes the decay of the population with the intrinsic LPPP rate  $k_0$  being the sum of the radiative and nonradiative decay rate. The second term accounts for the  $C_{60}$  concentration-dependent electron transfer. The last term considers bimolecular exciton annihilation processes.<sup>13</sup> The exciton dissociation due to the electron transfer leads to a transient buildup of the density of charge carriers  $N_{eh}$

$$\frac{\partial N_{eh}}{\partial t} = k_T(c)N_{S_1}. \quad (2)$$

The spatially separated charges have lifetimes exceeding the time-scale of our measurements. Thus, we neglect the back transfer (recombination) process that reduces the density of the charged excitations.

In order to be compared with the experimental data, the calculated transient densities  $N_{S_1,eh}$  have to be multiplied by their respective cross sections for transmission changes. The first step in the fitting procedure is to determine  $k_0$ , the bimolecular annihilation coefficient  $\gamma$  and the effective stimulated emission cross section from the SE transient of the undoped LPPP film. In agreement with our recent work on stimulated emission and gain narrowing in the same polymer, we find values of  $k_0^{-1} = 45$  ps and  $\gamma = 4.2 \times 10^{-9} \text{ cm}^3 \text{ s}^{-1}$ .<sup>13</sup> From fitting the transients for the molecularly doped samples we derive the concentration-dependent transfer rates  $k_T(c)$  and the cross section  $\sigma_{PIA}$  for the photoinduced absorption due to the charged species. The respective transfer times  $\tau_T = [k_T(c)]^{-1}$  decrease from 66 ps at 0.5%  $C_{60}$  to 5 ps at 5%  $C_{60}$ ,  $\sigma_{PIA}$  is determined to be  $4 \times 10^{-16} \text{ cm}^2$ .

In order to get a deeper insight into the underlying physics the experimentally determined transfer rates  $k_T(c)$  versus the fullerene concentration are plotted in the inset of Fig. 4. The observed linear dependence is compatible with a diffusion process preceding the dissociation.<sup>20,21,27</sup>

Microscopically, the diffusion is due to hopping of localized photoexcitations. The photogenerated excitons hop from one fully conjugated segment to a nearby segment either on the same chain or on another chain of the polymer. As soon as it reaches a site that is next to a  $C_{60}$  molecule the electron can transfer. A reasonable starting point for a more quantitative discussion is given by earlier work on energy transfer by exciton hopping in molecular crystals doped with guest molecules.<sup>20,22</sup> In the simplest form a constant hopping time  $\tau_h$ , being the average time spent by an exciton at a particular site, can be assumed. While the term *site* has a well-defined meaning for molecular crystals, it is much less clear in the case of conjugated polymers. The underlying fundamental problem that has not yet been fully resolved is the problem of the delocalization of the electronic states. There is, however, growing evidence that only a small number ( $n \leq 10$ ) of repeat units are coherently coupled.<sup>23,24</sup> Guided by earlier photoinduced absorption measurements<sup>25</sup> we assume that the conjugation length in LPPP amounts to eight phenyl rings.

In guest-host molecular crystals where energy transfer from a donating species to an accepting species occurs, the rate of energy transfer is simply given

$$k_T = (\tau_h)^{-1} \times \frac{c_G}{c_H}, \quad (3)$$

where  $c_G$  and  $c_H$  are the molecular concentrations of the guest and the host molecules. Hence, a plot of the transfer rate versus the molar concentration ratio  $c_G/c_H$  gives a straight line with a slope given by the inverse hopping time.

This model for *energy* transfer can be adapted to the case of *electron* transfer in  $C_{60}$ -doped conjugated polymers by assuming that the electron transfer to a specific fullerene molecule occurs only from one single-conjugated polymer segment in the direct neighborhood. This is rationalized by the fact that the electron transfer relies on spatial overlap of exponentially decaying electronic wave functions. The ET process itself occurs on a subpicosecond time scale, when the specific polymer site is occupied by an exciton. Based on these considerations the electron transfer rate is then given by

$$k_T = (\tau_h)^{-1} \frac{c_{C_{60}}}{c_{sites}}, \quad (4)$$

where  $c_{C_{60}}$  and  $c_{sites}$  are the molar concentrations of fullerene molecules and fully conjugated polymer segments, respectively. The predicted linear concentration dependence is in agreement with the experimentally found behavior in Fig. 4. From the slope we derive a hopping time of 1 ps, a value which is in agreement with previous estimates in the poly(p-phenylene vinylene) (PPV).<sup>26</sup> The total number of jumps of an exciton in the absence of the molecular dopant and for low-excitation pulse energies (low enough to avoid bimolecular annihilation processes) is  $n_h = \tau_0/\tau_h = 45$ . This enables us to estimate the exciton diffusion length  $L_D$  in LPPP. With  $d = (c_{sites})^{-1/3}$  as the typical distance of nearest neighbors  $L_D$  is calculated according to<sup>20</sup>

$$L_d = \frac{d\sqrt{n}}{\sqrt{3}}. \quad (5)$$

In our case, this yields a first estimate for the diffusion length  $L_d$  of  $\approx 6$  nm. In the following paragraph this value will be compared to the results of a more direct measurement of exciton diffusion in heterostructures of LPPP and a functionalized  $C_{60}$ .

## B. LPPP/ $C_{60}$ heterostructures

In order to investigate exciton dissociation in a more quantitative manner it is crucial to have a better control of the spatial distances involved. We have therefore fabricated LPPP/ $C_{60}$ -heterostructures comprising a self-assembled fullerene monolayer below a spin-coated LPPP film with various thicknesses. Figure 5 compares the emission spectra of an LPPP layer 35-nm thick with and without an adjacent fullerene monolayer. A strong reduction of the polymer PL due to the presence of the single fullerene monolayer is observed over the entire wavelength range. As discussed above for the blend systems, the PL quenching is not only due to a direct ET. Excitations that are generated far away from the interface have to diffuse prior to the dissociation process.

For a more detailed investigation of the involved diffusion and dissociation processes we now systematically study the thickness dependence of the PL quenching for the full set of samples exhibiting polymer film thicknesses between 5 and 65 nm.

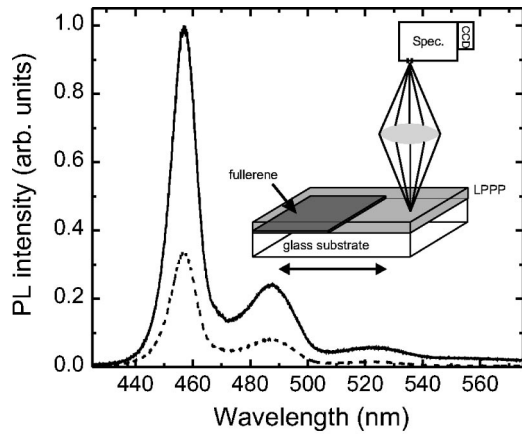


FIG. 5. PL spectra of a LPPP film 35-nm thick with (dashed line) and without (solid line) an adjacent self-assembled fullerene monolayer. The inset shows a sketch of the experimental setup. For excitation we use femtosecond laser pulses at 400 nm. The detection is accomplished with a spectrometer and a subsequent CCD camera.

The relative PL-quenching values  $\Delta I/I_0$  are depicted in Fig. 6 for the different polymer films. For the thinnest LPPP film (thickness 5 nm) the PL is almost totally quenched, whereas the PL of the thickest film investigated here (approximately 65 nm) is only reduced by 15%. The experimentally found thickness dependence of the PL quenching shown in Fig. 6 can be discussed in a simple model that accounts for the generation, the recombination, the diffusion, and the dissociation of excitons in the LPPP layer. For a quantitative analysis we use the following continuity equation for the temporally and spatially dependent density of photoexcitations  $n(z,t)$

$$\frac{\partial n(z,t)}{\partial t} = g(z,t) - k_0 n(z,t) - F(z)n(z,t) + D \frac{\partial^2 n(z,t)}{\partial z^2}. \quad (6)$$

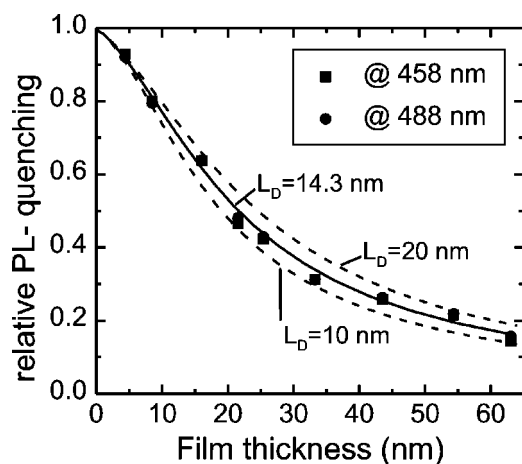


FIG. 6. The relative PL quenching of LPPP films with various thicknesses. The filled squares and circles are the experimental quenching values at different emission wavelengths. The solid line represents the calculation based on Eq. (6) and a diffusion length of 14 nm. For comparison we have included hypothetical curves for diffusion lengths of 10 and 20 nm, respectively.

Here,  $z$  is the distance from the fullerene/conjugated polymer interface and  $g(z,t)$  describes the generation process being proportional to the temporally and spatially dependent intensity of the femtosecond laser pulse. A Gaussian laser pulse with a full width at half maximum (FWHM) of 120 fs is assumed and the attenuation of the laser pulse during the penetration of the LPPP layer is taken into account. The second term on the right-hand side of Eq. (6) accounts for the superposition of radiative and nonradiative process that lead to a PL decay in the C<sub>60</sub>-free case. We have used a value of  $k_0^{-1} = \tau_0 = 45$  ps for the 1/e PL-decay time. The two last terms in Eq. (6) model the dissociation and the diffusion of photoexcitations, respectively. The dissociation process is described within a hopping ansatz with an exponential dependence of the rate for electron transfer between two localized states with overlapping wave functions

$$F(z) = f_0 \left( 1 + \frac{2z}{a} \right) e^{-(2z)/a}. \quad (7)$$

The simple exponential dependence has to be multiplied by the  $z$ -dependent prefactor shown in Eq. (7) which results from the integration of the transfer rates from one conjugated segment of the LPPP to all fullerene molecules at the interface. In Eq. (7),  $a$  describes the wave-function overlap of the electron donating polymer electronic state and the electron accepting state of the fullerene and  $f_0$  is a constant. If a reasonable value for  $a$  of less than 2 nm is assumed the thickness dependence of the PL quenching shown in Fig. 6 can only be understood if diffusion of excitations to the interface is taken into account. The solid line in Fig. 6 shows the good agreement that is found when a diffusion constant of  $D = 4.4 \times 10^{-2}$  cm<sup>2</sup>/s is assumed. Since this constant is related to the diffusion length via

$$L_D = \sqrt{D\tau_0}, \quad (8)$$

this comparison of the experimental data with the model calculations allows to determine the diffusion length to be  $L_D = 14$  nm. Albeit this value is of the same order of magnitude as the value of 6 nm estimated in the previous section it is significantly higher. Due to the more direct nature of the second measurement, we believe that the value deduced from the work on the heterostructures is much more reliable.

The smaller value for the exciton diffusion length found in the femtosecond measurements can be easily explained by the uncertainty in the concentration of polymer sites that act as donors in the ET to a fullerene molecule in the direct neighborhood. The most important contribution to this uncertainty is the delocalization length, which is not properly known. Other open questions are more related to the fullerene. We cannot rule out that more than one fullerene molecule form clusters in the polymer sample. Additionally, one can speculate that some of the C<sub>60</sub> molecules are only surrounded by sidegroups of the LPPP and are thus electronically not active. Further work using scanning probe microscopy techniques with high spatial resolution might give more insight into these issues.

It is also interesting to note that the value derived from our results on the heterostructures is larger than earlier estimates of 7 nm obtained by photocurrent experiments on heterostructures of PPV and C<sub>60</sub>.<sup>4</sup> This difference might be ex-

plained by the small inhomogeneous broadening in LPPP, which favors exciton diffusion. A larger value for the diffusion length of photoexcitations was estimated for poly(2,5-dioctyl-oxy-p-phenylene vinylene) (OO-PPV). This conclusion, however, was based on a strictly one dimensional model.<sup>27</sup>

The diffusion length we derived is surprisingly large, i.e., if the rather small exciton lifetime of only 45 ps in our LPPP is kept in mind. Since this value is most likely due to defect related nonradiative quenching processes one expects an even larger diffusion length for a defect free LPPP film where the lifetime is solely determined by the radiative decay. If we assumed a lifetime of 1 ns we would expect a diffusion length of more than 60 nm. Such high values would offer interesting prospects for heterojunction photovoltaic devices.

#### IV. SUMMARY AND CONCLUSION

In conclusion, we have investigated electron transfer processes in LPPP/C<sub>60</sub> composite systems. The quenching of the

photoluminescence and the stimulated emission of the polymer due to the ET to the electron accepting fullerene can be used for sensitive measurements. Femtosecond pump/probe experiments have directly revealed the timescale of the ET to C<sub>60</sub>. For fullerene concentrations between 0.5% and 5% the electron is transferred within 66 and 5 ps, respectively. The concentration dependence can be explained by exciton diffusion occurring prior to the electron transfer process itself. The diffusion length of excitons in LPPP was quantitatively measured in well-defined LPPP/C<sub>60</sub> heterostructures consisting of a self-assembled fullerene monolayer and a spin-coated LPPP film. We deduce a value of 14 nm.

#### ACKNOWLEDGMENTS

It is a pleasure to acknowledge O. Holderer and M. Perner for their contributions and W. Stadler for excellent technical support. We thank T. Salditt and M. Vogel for x-ray reflectivity measurements. This work was financially supported by the DFG through Sonderforschungsbereich 377 and the BMBF via Project No. 13N6821 6.

- <sup>1</sup>N. S. Sariciftci, *Prog. Quantum Electron.* **19**, 131 (1995).
- <sup>2</sup>C. H. Lee, G. Yu, D. Moses, K. Pakbaz, C. Zhang, N. S. Sariciftci, A. J. Heeger, and F. Wudl, *Phys. Rev. B* **48**, 15 425 (1993).
- <sup>3</sup>X. Wei, Z. V. Vardeny, N. S. Sariciftci, and A. J. Heeger, *Phys. Rev. B* **53**, 2187 (1996).
- <sup>4</sup>J. J. M. Halls, K. Pichler, R. H. Friend, S. C. Moratti, and A. B. Holmes, *Appl. Phys. Lett.* **68**, 3120 (1996).
- <sup>5</sup>S. Morita, A. Zakhidov, and K. Yoshino, *Solid State Commun.* **82**, 249 (1992).
- <sup>6</sup>B. Kraabel, D. McBranch, N. S. Sariciftci, D. Moses, and A. J. Heeger, *Phys. Rev. B* **50**, 18 543 (1994).
- <sup>7</sup>B. Kraabel, J. C. Hummelen, D. Vacar, D. Moses, N. S. Sariciftci, A. J. Heeger, and F. Wudl, *J. Chem. Phys.* **104**, 1 (1996).
- <sup>8</sup>D. Vacar, E. Maniloff, D. McBranch, and A. Heeger, *Phys. Rev. B* **56**, 4573 (1997).
- <sup>9</sup>G. Decher, J. Hong, and J. Schmitt, *Thin Solid Films* **210/211**, 831 (1992).
- <sup>10</sup>C. Kallinger, A. Haugeneder, U. Lemmer, J. Feldmann, H. Hong, M. Tarabia, D. Davidov, E. Harth, M. Walter, U. Scherf, A. Gügel, and K. Müllen, in *Molecular Nanostructures*, edited by H. Kuzmany, J. Fink, M. Mehring, and S. Roth (World Scientific, Singapore, 1997), pp. 515-518.
- <sup>11</sup>F. Hide, M. A. Diaz-Garcia, B. J. Schwartz, M. R. Andersson, Pei Qibing, and A. J. Heeger, *Science* **273**, 1833 (1996).
- <sup>12</sup>A. Haugeneder, M. Hilmer, C. Kallinger, M. Perner, W. Spirkel, U. Lemmer, J. Feldmann, and U. Scherf, *Appl. Phys. B: Lasers Opt.* **66**, 389 (1998).
- <sup>13</sup>A. Haugeneder, M. Neges, C. Kallinger, W. Spirkel, U. Lemmer, J. Feldmann, and U. Scherf, *J. Appl. Phys.* (to be published).
- <sup>14</sup>U. Jonas, F. Cardullo, P. Belik, F. Diederich, A. Gügel, E. Harth, A. Herrmann, L. Isaacs, K. Müllen, H. Ringsdorf, C. Thilgen, P. Uhlmann, A. Vasella, C. A. A. Waldraff, and M. Walter, *Chem.-Eur. J.* **1**, 243 (1995).
- <sup>15</sup>C. Schlebusch, B. Kessler, S. Cramm, and W. Eberhardt, *Synth. Met.* **77**, 151 (1996).
- <sup>16</sup>J. Sturm, S. Tasch, A. Niko, G. Leising, E. Toussaere, J. Zyss, T. C. Kowalczyk, K. D. Singer, U. Scherf, and J. Huber, *Thin Solid Films* **298**, 138 (1997).
- <sup>17</sup>Due to orientational relaxation slight differences in the picosecond dynamics are observed for different polarizations of the probe pulses. The final results for the electron transfer rates discussed here, however, do not depend on the polarization of the probe beam with respect to the pump beam.
- <sup>18</sup>T. Pauck, R. Hennig, M. Perner, U. Lemmer, U. Siegner, R. F. Mahrt, U. Scherf, K. Müllen, H. Bässler, and E. O. Göbel, *Chem. Phys. Lett.* **244**, 171 (1995).
- <sup>19</sup>M. Yan, L. J. Rothberg, F. Papadimitrakopoulos, M. E. Galvin, and T. M. Miller, *Phys. Rev. Lett.* **72**, 1104 (1994).
- <sup>20</sup>W. Klöpffer, in *Electronic Properties of Polymers*, edited by G. Pfister (Wiley, New York, 1982), pp. 162-213.
- <sup>21</sup>S. V. Frolov, P. A. Lane, M. Ozaki, K. Yoshino, and Z. V. Vardeny, *Chem. Phys. Lett.* **286**, 21 (1998).
- <sup>22</sup>M. Pope, *Electronic Processes in Organic Crystals* (Oxford University Press, Oxford, 1982).
- <sup>23</sup>U. Rauscher, H. Bässler, D. D. C. Bradley, and M. Hennecke, *Phys. Rev. B* **42**, 9830 (1990).
- <sup>24</sup>U. Lemmer and E. Göbel, in *Nature of the Primary Photoexcitation in Conjugated Polymers*, edited by N. Sariciftci (World Scientific, Singapore, 1997), pp. 211-253.
- <sup>25</sup>W. Graupner, M. Mauri, J. Stampfl, G. Leising, U. Scherf, and K. Müllen, *Solid State Commun.* **91**, 7 (1994).
- <sup>26</sup>M. Scheidler, U. Lemmer, R. Kersting, S. Karg, W. Riess, B. Cleve, R. F. Mahrt, H. Kurz, H. Bässler, E. O. Göbel, and P. Thomas, *Phys. Rev. B* **54**, 5536 (1996).
- <sup>27</sup>K. Yoshino, Yin Xiao Hong, K. Muro, S. Kiyomatsu, S. Morita, A. A. Zakhidov, T. Noguchi, and T. Ohnishi, *Jpn. J. Appl. Phys., Part 2* **32**, L357 (1993).